

## BeO $\mu$ calorimeter for the ${}^7\text{Be}$ electron capture decay measurement

M. Galeazzi, F. Gatti, P. Meunier, and S. Vitale

*INFN of Genoa and Genoa University, Via Dodecaneso 33, I-16146 Genoa, Italy*

(Received 8 July 1997)

${}^7\text{Be}$  electron capture decay to  ${}^7\text{Li}$  has been investigated by means of a cryogenic  $\mu$  calorimeter. A cryogenic particle detector, due to its low energy threshold and good energy resolution, allows us to detect for the first time the complete  ${}^7\text{Be}$  calorimetric energy spectrum with a peak width of 24 eV full width at half maximum at 112 eV. The observed decrease in the rate of the absorber activity corresponds to the expected  ${}^7\text{Be}$  half-life of 53 days. This kind of detector has an important application in the environment of a lithium radiochemical solar neutrino experiment which is in progress in Moscow. A discussion about the possible processes which take place inside the BeO absorber during the energy thermalization is reported. [S0556-2813(98)02404-2]

PACS number(s): 23.40.-s, 07.20.Mc, 29.40.Vj, 26.65.+t

### I. INTRODUCTION

The  ${}^7\text{Be}$  nucleus decays by means of electron capture to  ${}^7\text{Li}$ . In 89.6% of the decays the  ${}^7\text{Be}$  nucleus goes to the  ${}^7\text{Li}$  ground state, while in 10.4% of the decays the  ${}^7\text{Be}$  nucleus goes to a 478 keV excited state [1]. The decay to the ground state has a maximum detectable energy of 112 eV, which is the limit for the traditional detection techniques. Until now the principal measurements of this decay have been performed detecting only a limited fraction of the total decays [2,3]. Cryogenic detectors, due to the low energy threshold and good energy resolution, can detect energies less than 100 eV [4]; besides both electromagnetic and nuclear recoil energy releases can be detected [5,6]. This allows the direct investigation of  ${}^7\text{Be}$  decay to the  ${}^7\text{Li}$  ground state.

Measurement of the  ${}^7\text{Be}$  electron capture decay with a counting efficiency close to 100% is an essential result for the development of a lithium solar neutrino experiment which is in progress in Moscow [7]. The experimental project is to install 10 tons of lithium deep underground as a solar neutrino target. The flux measurement has to be performed counting the  ${}^7\text{Be}$  isotopes produced in the target by neutrino capture. The expected count rate of the  ${}^7\text{Be}$  extracted from the target is about 0.5–2.5 counts per day for a counting efficiency of approximately 90% and a total number of counts (for a counting time of 5 half-lives of  ${}^7\text{Be}$ ) between 35 and 175 [8]. The conventional counting technique can detect only the 478 keV  $\gamma$  ray emitted after the decay of  ${}^7\text{Be}$  to the  ${}^7\text{Li}$  excited state (branching ratio = 10%). This limits the counting efficiency to about 8%; therefore the mass of the lithium target should be about 100 tons, which is very expensive and very difficult to realize.

We already showed that the 112 eV  ${}^7\text{Be}$  decay line can be detected by means of a cryogenic  $\mu$  calorimeter with a beryllium metal absorber; an energy resolution of 53 eV full width at half maximum (FWHM) at 112 eV has been obtained [9]. We decided to use a metal absorber because preliminary tests in Moscow have shown that Be metal can be extracted with a high efficiency and high purity level from the lithium tank [7,8].

It has to be noted that a metal absorber is not the optimal choice for a microcalorimeter detector, because of the high

heat capacity of metal compared with a superconducting or a dielectric absorber. In order to improve the detector performance it is possible to use different beryllium chemical compounds as absorbers. One such material, which is presently under investigation in Moscow as a possible alternative final solid form in which Be can be extracted from the lithium, is BeO [7,8]. The dielectric properties of this material make it more suitable as a detector absorber with respect to the beryllium metal.

A  $\mu$  calorimeter using a BeO absorber has been developed, with the goal of measuring the  ${}^7\text{Be}$  electron capture decay with a low energy threshold and good energy resolution, in order to detect all the  ${}^7\text{Be}$  low energy release (Auger electron plus the nuclear recoil), which goes from 28.5 eV to 112 eV.

### II. ${}^7\text{Be}$ ELECTRON CAPTURE DECAY

In Fig. 1 the  ${}^7\text{Be}$  decay scheme is shown.  ${}^7\text{Be}$  decays by means of a superallowed electron capture (EC) transition to  ${}^7\text{Li}$ . Both  $K$ -capture and  $L$ -capture are energetically allowed, and the EC relative probabilities can be theoretically calculated [10]. In Table I the probability values and the detectable energies following each decay branch are reported.

Up to now, the measurements of  ${}^7\text{Be}$  electron capture decay have been performed with traditional  $\gamma$ -ray detectors like NaI scintillators [2] or Ge(Li) spectrometers [3] to measure the inner bremsstrahlung probabilities and end-point

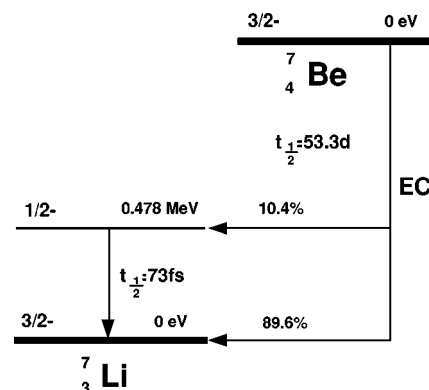


FIG. 1. The  ${}^7\text{Be}$  electron capture decay scheme.

TABLE I. Expected detectable energy release and branching ratio for the  ${}^7\text{Be}$  electron capture energy spectrum.

		${}^7\text{Be}\rightarrow{}^7\text{Li}$			${}^7\text{Be}\rightarrow{}^7\text{Li}^*$		
		Energy	Total energy	Probability	Energy	Total energy	Probability
$K$ capture	Auger	55 eV			55 eV		
	Electrons		112 eV	78.8%		83.5 eV	9.4%
	Nuclear recoil	57 eV			28.5 eV		
$L$ capture	Auger	-			-		
	Electrons		57 eV	11%		28.5 eV	0.8%
	Nuclear recoil	57 eV			28.5 eV		

values. Specific experiments for the nuclear recoil energy measurement have been performed too [11,12]. These detection techniques have the intrinsic limit of a small efficiency, which excludes the use of these methods in the Moscow solar neutrino experiment with a 10-ton lithium target [8].

In a calorimetric measurement of an energy spectrum it is possible to detect both electromagnetic and nuclear recoil energies [5,6,13]; the only limit on the electromagnetic energy detection is given by the absorption length in the absorber material and therefore by the detector dimension. Moreover, because of the low energy threshold and good energy resolution, a cryogenic particle detector, in principle, may have a 100% detection efficiency.

In the case of the decay to the lithium excited state electron capture decay is followed, with a half-life of 73 fs, by the emission of a 478 keV  $\gamma$  ray [1]. Therefore there are two nuclear recoils, one after the neutrino emission and the other after the  $\gamma$ -ray emission, with a theoretical total energy of 28.5 eV.

Thus the total nuclear recoil energy depends on the difference between the  ${}^7\text{Li}$  excited state half-life and the stopping time of the nucleus following neutrino emission. If the nucleus stopping time is longer than the  ${}^7\text{Li}$  excited state half-life, the recoil energy spectrum has a continuous distribution from 0 eV to 28.5 eV instead of a  $\delta$ -like peak distribution. The expected sound velocity in the BeO absorber supports this second hypothesis; it should be interesting to directly verify it with a good detector.

### III. EXPERIMENTAL APPARATUS

The general design of a  $\mu$  calorimeter has already been reported by many authors [5]. The present  $\mu$  calorimeter [14] consists of a 3  $\mu\text{g}$  absorber of BeO linked using epoxy with a neutron transmutation doped (NTD) germanium thermistor (50  $\mu\text{m}\times 100\ \mu\text{m}\times 200\ \mu\text{m}$ ) as sensor. The beryllium oxide sample has been previously irradiated with 100 MeV protons at the Moscow Meson Facility in order to produce the  ${}^7\text{Be}$  isotope inside. The beryllium absorber was obtained by cutting in very small pieces a BeO single crystal after the irradiation in order to have the activity adequate for a cryogenic detector (a few Bq). The evaluation of the activity was performed measuring the intensity of the 478 keV  $\gamma$  line using a low background HPGe detector at Moscow.

The detector is installed in a dilution refrigerator at an operating temperature of about 45 mK. A thermal connection

to the refrigerator mixing chamber and electrical connections to the source follower, placed inside the refrigerator, are provided by two ultrasonic bonded 15  $\mu\text{m}$  aluminum wires. Although the amount of energy is very small (only 112 eV in this case), the increase in temperature is not negligible (in the range of  $\mu\text{K}$ ) due to an extremely small heat capacity of the  $\mu$  calorimeter at the working temperature.

The signal is read off using a low noise preamplifier (1 nV/ $\sqrt{\text{Hz}}$ ) working at a temperature of about 100 K installed inside the cryostat, together with a room temperature amplifier also used as antialiasing filter for the analog-to-digital (A/D) conversion. The conversion is made using a Camac wave form recorder (LeCroy 6810) controlled by a Digital VAX station through a crate controller 3929 from Kinetics System. The data are recorded on the VAX station disk for an off-line analysis using digital signal processing [15].

The off-line analysis can be performed in three different ways: by integration of the pulses, by optimum filtering, or by adaptative filtering; the efficiency of the methods depends on the characteristics of the thermal pulses and of the noise. The optimum filter consists of a convolution of each pulse with a reference pulse built averaging ‘‘good pulses’’ (at least 30) which have to be selected visually without pileup and noise spikes [16]. The adaptative filter is a traditional digital adaptative filter using the reference pulse built for the optimum filter as the reference channel [17]. In the experiment all three methods were employed independently, and produced the same results.

For each pulse rise time, the pretrigger slope and noise, decay time, and chi-square test are also computed for a complete analysis using PAW [18]. The pulses have a very definite shape: a relatively fast rise time (less than 1 ms) followed by a slow slope (a few tens of ms) (see Fig. 2), which enables us to discriminate the noise by pulse shape analysis using  $\chi^2$ .

The energy calibration is provided by an external removable x-ray source of  ${}^{55}\text{Fe}$  (5898 eV and 6490 eV x rays). Taking into account the relative dimension of the detector absorber and of the thermistor, and the relative absorption probability for  ${}^{55}\text{Fe}$  x rays, the interaction probability of x rays into the detector thermistor is about 6 times higher than the interaction probability into the BeO absorber.

The shape of the pulses due to the x-ray absorption into the two detector parts is rather different; the different shape of the thermal pulse due to a direct interaction in a thermistor

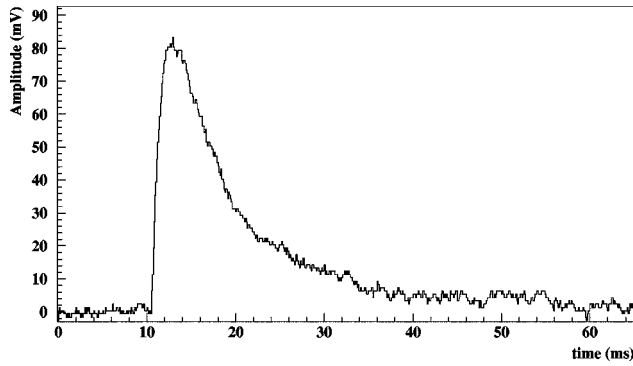


FIG. 2. A 112 eV pulse shape; it is possible to calculate a base line noise of 5 eV FWHM.

is a known effect, which has already been studied and explained [19]. The pulse shape analysis allows us to distinguish between the two different kinds of pulses with a confidence level of  $3\sigma$ . In our measurement we have identified two sets of calibration lines; the most intense pulses can be attributed to the interaction of the 5898 eV and 6490 eV x rays in the germanium thermistor, the weaker ones to the x-ray interaction in the beryllium oxide. The count rate of the x rays interacting with the BeO absorber has been found to be  $(0.013 \pm 0.003)$  Hz, and the count rate into the NTD Ge thermistor is  $(0.075 \pm 0.004)$  Hz; this is in good agreement with the expected probability ratio.

The relative position of the two  ${}^{55}\text{Fe}$  spectral lines in BeO does not show any evidence of a detector nonlinearity within  $1\sigma$ . The linearity of a cryogenic particle detector below 10 keV has been already affirmed by many authors [4,20].

#### IV. EXPERIMENTAL RESULTS

In Fig. 3 the calorimetric spectrum of  ${}^7\text{Be}$  electron capture decay has been reported (solid line). Comparing the data recorded in different runs (with slightly different working conditions), we found that the position of the higher peak of Fig. 3 is  $(118 \pm 3)$  eV with a difference of 5% with respect to the  ${}^7\text{Be}$  expected energy of 112 eV. The energy width of this peak is 24 eV FWHM.

In Fig. 3 it is also possible to identify a second contribution, at lower energy, that we ascribe to  $L$  electron capture to

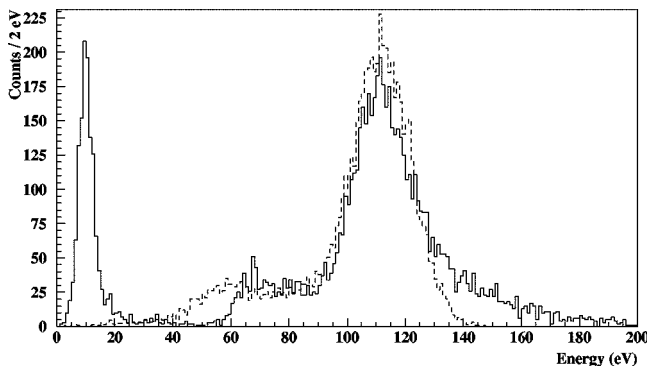


FIG. 3. The  ${}^7\text{Be}$  energy spectrum; the solid line represents the measured spectrum; the dotted line represents a Monte Carlo simulation assuming a complete energy thermalization efficiency of the detector.

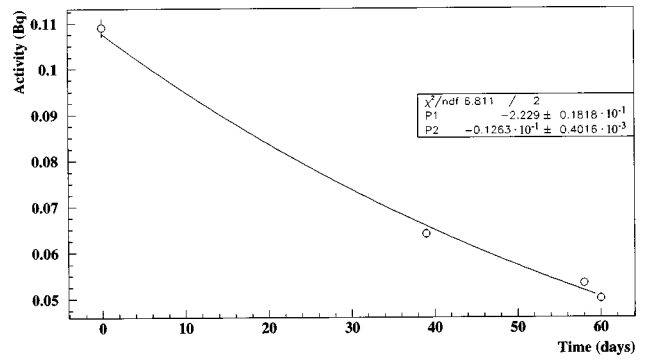


FIG. 4. The count rate of pulses between 50 eV and 150 eV versus time; the measured half-life is  $(55 \pm 2)$  days, which is in agreement with the  ${}^7\text{Be}$  half-life of 53 days.

the  ${}^7\text{Li}$  ground state plus the  $K$  electron capture decay to the  ${}^7\text{Li}$  excited state. The 478 keV  $\gamma$  rays following the decay to the  ${}^7\text{Li}$  excited state cannot be detected by our detector, due to the negligible detector size with respect to the absorption length at this energy.

The activity of the pulses with an energy between 20 eV and 150 eV at the time of the first measurement was  $(0.109 \pm 0.002)$  Hz. In order to verify that the pulses with this measured energy release correspond to  ${}^7\text{Be}$  decay, the measurement was repeated after 39, 58, and 60 days; the two last measurements have been performed without the  ${}^{55}\text{Fe}$  calibration source, using a self-calibration of the 112 eV peak. The measured half-life is  $\tau_{1/2} = (55 \pm 2)$  days (see Fig. 4), which is in good agreement with the  ${}^7\text{Be}$  expected one of  $(53.29 \pm 0.02)$  days [1].

A Monte Carlo simulation of the  ${}^7\text{Be}$  calorimetric spectrum, assuming a 100% thermalization efficiency and taking into account the measured energy resolution and the data reported in Table I, has been realized. The comparison between the Monte Carlo simulation and the real data is reported in Fig. 3 (dotted line). Notice that the distance between the two detectable peaks in the real case is different from the expected one; this fact can be explained either by a detector nonlinearity (in contradiction with the considerations about the energy calibration reported in Sec. III) or by a higher energy thermalization efficiency for the nuclear recoil energy release with respect to the electromagnetic one.

A thermalization efficiency of the electromagnetic energy release less than 100% and lower with respect to the thermalization efficiency of the nuclear recoil energy, in a dielectric or semiconductor detector absorber, has already been measured and studied by many authors (see, for example, [13] and [21]).

In our measurement there is also other experimental evidence which has to be investigated. For instance in Fig. 2, the base line noise equals 5 eV FWHM, i.e., about 5 times less than the measured width of the 112 eV line; the corresponding signal-to-noise ratio is approximately 20.

Moreover, in the spectrum reported in Fig. 3 it is possible to note two characteristic effects, an asymmetric shape of the 112 eV spectral line with a tail in the high energy direction and the existence of a peak with an energy of about 10 eV.

We investigate first the origin of the 10 eV pulses. A careful investigation of the full wave form recorded was performed to be sure that the events in this peak were due to real

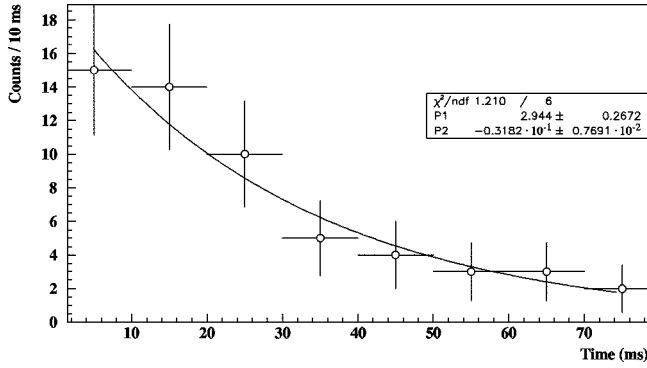


FIG. 5. Temporal correlation of a sample of 10 eV pulse couples; the correlation time is equal to  $(31 \pm 8)$  ms.

thermal pulses and not to noise spikes. We verified their characteristics analyzing a sample of 1000 pulses for each run, for a total of 4000 pulses. The results of this analysis are the following.

(i) The decreasing versus the time of the count rate of these pulses is compatible within one sigma with the  ${}^7\text{Be}$  half-life.

(ii) The ratio between their count rate and the  ${}^7\text{Be}$  count rate is  $(1.6 \pm 0.3)$ .

(iii) The analysis shows that in several cases two 10 eV pulses are emitted within a time interval smaller than 80 ms; the analysis of the time interval between the pulses for a sample of couples is shown in Fig. 5; our experimental apparatus does not allow the investigation of the possible time correlation between  ${}^7\text{Be}$  pulses and 10 eV pulses.

(iv) The characteristics of the 10 eV pulses shown before are apparently independent of the presence of the  ${}^{55}\text{Fe}$  calibration source; as already pointed out, the rate of the  ${}^{55}\text{Fe}$  x rays interacting in the BeO absorber is too low with respect to the  ${}^7\text{Be}$  rate in order to verify a consequent increase of the 10 eV pulse count rate.

The reported results point out the existence of a correlation between the  ${}^7\text{Be}$  decay thermal pulses and the 10 eV pulses; each  ${}^7\text{Be}$  pulse can be related to the emission of the small pulses: on average there are  $(1.6 \pm 0.3)$  pulses for each  ${}^7\text{Be}$  thermal pulse. When a couple of pulses is emitted, these seem to be emitted with a correlation time of  $(31 \pm 8)$  ms (see Fig. 5).

All this experimental evidence might be explained by the existence of metastable states of about 10 eV which could be excited in the thermalization process of the electromagnetic energy release following the  ${}^7\text{Be}$  decay.

Using a Monte Carlo simulation we have checked that the above hypothesis of excitation of the metastable states is in agreement with the experimental energy spectrum (see Fig. 6), and can thus explain the fact that the 112 eV peak width is worse than expected from the detector noise.

In this simulation we assumed that the electromagnetic energy release is completely converted into electron-hole pairs: Since 17 eV are needed to create each pair, only three pairs are created. These pairs can rapidly recombine into phonons or can be trapped in 10 eV metastable states according to a binomial distribution with a recombination probability of 0.39 (which gives the measured mean value of the number of metastable states of 1.6). The detected energy is then equal to the total energy release minus the energy

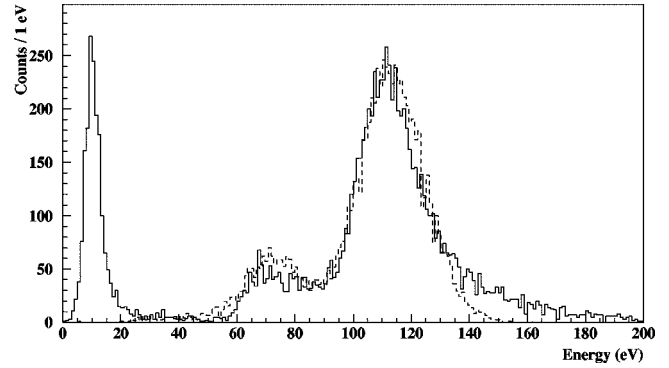


FIG. 6. The  ${}^7\text{Be}$  energy spectrum; the solid line represents the measured spectrum; the dotted line represents a Monte Carlo simulation taking into account electromagnetic energy trapping.

trapped in the metastable states. The contribution of the base line noise has been superimposed onto the thermalized energy distribution obtained as above explained; the energy resolution is then determined by the combination of the base line noise and the metastable state distribution.

The trapping effect of a part of the electromagnetic energy release is in agreement with the difference of 5% in the spectrum energy calibration and with the difference between the signal-to-noise ratio and the measured peak widths.

An interesting point, already mentioned in Sec. II, is that the  ${}^7\text{Be}$  spectrum shape depends on the difference between the  ${}^7\text{Li}$  excited state half-life and the stopping time of the nucleus following the neutrino emission. In order to investigate which processes take place in our detector after the  ${}^7\text{Be}$   $K$  capture to the  ${}^7\text{Li}$  excited state, we compared the acquired spectrum with a simulation of both the extreme cases ( $\delta$ -like peak and  $\gamma$ - $\nu$  angle depending energy spectrum) using a  $\chi^2$  test (see Fig. 7). In the simulation the contribution of metastable states is also taken into account. We found that the experimental spectrum shape is compatible with a  $\delta$ -like peak energy release within one  $\sigma$  ( $\chi^2=1.1$ ); the experimental spectrum shape is instead compatible with a  $\gamma$ - $\nu$  angle depending energy release of the same decay with a probability smaller than 1% ( $\chi^2=3.7$ ). We have also seen that this result is practically independent of the parameter of the

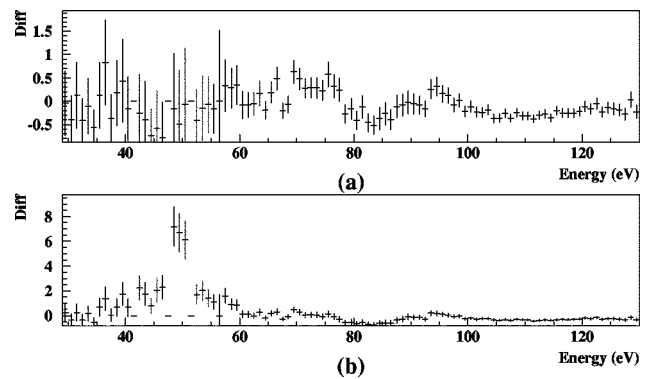


FIG. 7. Comparison between real data and Monte Carlo simulation in the case of a  ${}^7\text{Be}$   $K$  capture to a  ${}^7\text{Li}$  excited state following a  $\delta$ -like distribution (a) and in the case of a  $\gamma$ - $\nu$  angle depending energy spectrum (b); the plotted parameter is  $\text{Diff} = (N_{\text{Monte Carlo}} - N_{\text{real}}) / N_{\text{real}}$ .

metastable state binomial distribution in the Monte Carlo simulation.

As expected from theoretical calculations, with this experimental result we can then conclude that the  $^7\text{Be}$  energy calorimetric spectrum is composed of three  $\delta$ -like peaks. Hence we may assume, in Fig. 6, that the contribution at lower energy corresponds to the sum of two peaks, one due to the  $^7\text{Be}$   $L$ -capture to the  $^7\text{Li}$  ground state and the other due to the  $^7\text{Be}$   $K$  capture to the  $^7\text{Li}$  excited state convoluted with a Gaussian distribution due to the detector energy resolution.

## V. CONCLUSION

The  $^7\text{Be}$  electron capture decay to  $^7\text{Li}$  has been successfully detected by means of a cryogenic  $\mu$  calorimeter. Thanks to the low energy threshold and to the good energy resolution, it has been possible to detect for the first time the complete  $^7\text{Be}$  calorimetric energy spectrum with a peak width of 24 eV FWHM at 112 eV. The total detectable energy release (Auger electron plus the nuclear recoil energy), following the  $K$  and  $L$  electron capture, goes from 28.5 eV to 112 eV. The observed decrease in the rate of the absorber activity is  $\tau_{1/2} = (55 \pm 2)$  days, which is in agreement with the expected  $^7\text{Be}$  half-life of 53 days.

This is an essential result as the detection of  $^7\text{Be}$  decay with an efficiency close to 100% was the principal obstacle to realizing a lithium solar neutrino experiment.

The analysis of the experimental results and their comparison with a Monte Carlo simulation give new important information to investigate the thermalization processes which take place inside a dielectric material. This measurement is the starting point for a complete systematic study of the thermalization processes using different absorber materials and different radiation sources (Auger electron, x rays, and neutral particles).

In the future, with a good detector sensitivity and a high statistic measurement, the study of  $^7\text{Be}$  EC decay using different absorber materials could be also interesting in order to investigate the chemical atomic bonding influence on the decay properties [22,23].

## ACKNOWLEDGMENTS

We want to thank Dr. A. V. Kopylov and Dr. E. A. Yanovich from INR of Moscow for the irradiation of BeO samples and for helpful discussions and suggestions. This work was supported by INFN and by the EC-HCM Program ‘‘Cryogenic Detectors,’’ Contract No. ERB-CHRXCT930341.

- 
- [1] E. Bowne, J. M. Dairiki, and R. E. Doebler, in *Table of Isotopes*, edited by C. M. Lederer (Wiley, New York, 1978) p. 3.
  - [2] B. I. Persson and S. E. Koonin, *Phys. Rev. C* **5**, 1443 (1972).
  - [3] M. Mutterer, *Phys. Rev. C* **8**, 2089 (1973).
  - [4] F. Fontanelli, M. Galeazzi, F. Gatti, P. Meunier, A. Swift, and S. Vitale, *Nucl. Instrum. Methods Phys. Res. A* **370**, 373 (1996).
  - [5] N. Booth, B. Cabrera, and E. Fiorini, *Annu. Rev. Nucl. Part. Sci.* **46**, 471 (1996).
  - [6] A. Alessandrello *et al.*, *J. Low Temp. Phys.* **93**, 201 (1993).
  - [7] A. V. Kopylov, in *Proceedings of the 4th International Solar Neutrino Conference, Heidelberg, 1997* (unpublished); P. Meunier, *ibid.*; M. Galeazzi, in *Proceedings of the 9th International School on Particles and Cosmology, Baksan, 1997* (unpublished).
  - [8] M. Galeazzi, G. Gallinaro, F. Gatti, P. Meunier, S. Vitale, A. V. Kopylov, V. V. Petukhov, E. A. Yanovich, and G. T. Zatsopin, *Phys. Lett. B* **398**, 187 (1997).
  - [9] M. Galeazzi, G. Gallinaro, F. Gatti, P. Meunier, S. Vitale, A. V. Kopylov, and E. A. Yanovich, *Nucl. Instrum. Methods Phys. Res. A* **401**, 317 (1997).
  - [10] W. Bambynek, H. Behrens, M. H. Chen, B. Crasemann, M. L. Fitzpatrick, K. W. D. Ledingham, H. Genz, M. Mutterer, and R. L. Intemann, *Rev. Mod. Phys.* **49**, 77 (1977).
  - [11] P. B. Smith and J. S. Allen, *Phys. Rev.* **81**, 381 (1950).
  - [12] R. Davis, Jr., *Phys. Rev.* **86**, 976 (1952).
  - [13] T. Shutt *et al.*, *Nucl. Instrum. Methods Phys. Res. A* **370**, 165 (1996).
  - [14] P. Meunier, Ph.D. thesis, University of Genoa, 1997.
  - [15] E. Cosulich, F. Fontanelli, G. Gallinaro, F. Gatti, A. M. Swift, and S. Vitale, *Nucl. Phys.* **A592**, 59 (1995).
  - [16] E. Cosulich and F. Gatti, *Nucl. Instrum. Methods Phys. Res. A* **321**, 211 (1992).
  - [17] F. Gatti and A. Nostro, *Nucl. Instrum. Methods Phys. Res. A* **368**, 765 (1996).
  - [18] PAW (Physical Analysis Workstation), CERN Program Library entry Q121, Geneva 1995.
  - [19] F. Pröbst, M. Frank, S. Cooper, P. Colling, D. Dummer, P. Ferger, G. Forster, A. Nucciotti, W. Seidel, and L. Stodolsky, *J. Low Temp. Phys.* **100**, 69 (1995).
  - [20] D. McCammon, W. Cui, M. Juda, J. Morgenthaler, J. Zhang, R. L. Kelley, S. S. Holt, G. M. Madejski, S. H. Moseley, and A. E. Szymkowiak, *Nucl. Instrum. Methods Phys. Res. A* **326**, 157 (1983).
  - [21] D. McCammon, M. Juda, J. Zhang, R. L. Kelley, S. H. Moseley, and A. E. Szymkowiak, *IEEE Trans. Nucl. Sci.* **33**, 236 (1986).
  - [22] E. Segré, *Phys. Rev.* **71**, 274 (1947).
  - [23] J. J. Kraushaar, E. D. Wilson, and K. T. Bainbridge, *Phys. Rev.* **90**, 610 (1953).